

Deciphering the Roles of Outer Membrane Protein A Extracellular Loops in the Pathogenesis of *Escherichia coli* K1 Meningitis^{*[5]}

Received for publication, August 24, 2010, and in revised form, October 5, 2010. Published, JBC Papers in Press, November 11, 2010, DOI 10.1074/jbc.M110.178236

Rahul Mittal[‡], Subramanian Krishnan[‡], Ignacio Gonzalez-Gomez[§], and Nemani V. Prasadarao^{‡¶||1}

From the [‡]Division of Infectious Diseases, Department of Pediatrics, and Departments of [§]Pathology and [¶]Surgery, ^{||}Saban Research Institute, Childrens Hospital Los Angeles and Keck School of Medicine, University of Southern California, Los Angeles, California 90027

Outer membrane protein A (OmpA) has been implicated as an important virulence factor in several Gram-negative bacterial infections such as *Escherichia coli* K1, a leading cause of neonatal meningitis associated with significant mortality and morbidity. In this study, we generated *E. coli* K1 mutants that express OmpA in which three or four amino acids from various extracellular loops were changed to alanines, and we examined their ability to survive in several immune cells. We observed that loop regions 1 and 2 play an important role in the survival of *E. coli* K1 inside neutrophils and dendritic cells, and loop regions 1 and 3 are needed for survival in macrophages. Concomitantly, *E. coli* K1 mutants expressing loop 1 and 2 mutations were unable to cause meningitis in a newborn mouse model. Of note, mutations in loop 4 of OmpA enhance the severity of the pathogenesis by allowing the pathogen to survive better in circulation and to produce high bacteremia levels. These results demonstrate, for the first time, the roles played by different regions of extracellular loops of OmpA of *E. coli* K1 in the pathogenesis of meningitis and may help in designing effective preventive strategies against this deadly disease.

Escherichia coli K1 is a prominent Gram-negative bacterium that causes meningitis in neonates with case fatality rates ranging from 5 to 30% of infected infants (1–4). Those who survive are often left with permanent neurological dysfunction such as hearing loss, mental retardation, and cortical blindness (5, 6). Despite the use of advanced antibiotics, the morbidity and mortality rates associated with *E. coli* K1 meningitis remain unchanged over the last few decades (7, 8). In addition, because of a recent surge in antibiotic-resistant *E. coli* K1 strains, the mortality rates will further increase significantly (9, 10). Therefore, new modes of prevention are warranted for which the understanding disease pathophysiol-

ogy is clearly necessary. Studies from this laboratory have demonstrated that *E. coli* K1 interacts with human brain microvascular endothelial cells (HBMEC)² to enter the central nervous system (11, 12). The interaction of the bacterium with HBMEC is mediated by outer membrane protein A (OmpA) of *E. coli* K1 and a glycoprotein receptor, Ecgp96, on HBMEC (13, 14). OmpA initially binds to GlcNAc1–4GlcNAc epitopes of Ecgp96, followed by the peptide portion of the receptor (15). Of note, synthetic peptides that represent loops 1 and 2 of OmpA prevented the *E. coli* K1 invasion of HBMEC (15). OmpA has been shown to be responsible for conferring serum resistance by binding to a complement regulator protein, C4b-binding protein (C4bp) (16, 17). Neonates having lower than the threshold levels of C4bp may be at a higher risk to *E. coli* K1 meningitis as evidenced when the bacterium treated with adult serum, which contained higher amounts of C4bp, could not invade HBMEC compared with newborn serum treatment (18). Nonetheless, neither of the sera prevents the entry of *E. coli* K1 into macrophages or dendritic cells (DCs) for which OmpA expression is also needed, indicating that various epitopes of OmpA are involved at different stages of pathogenesis of *E. coli* K1 meningitis (19, 20). Therefore, in this study it is our goal to delineate the roles of different domains of OmpA interacting with various cells *in vitro* and their role in a well established newborn mouse model of meningitis (7, 21–23).

OmpA is a highly conserved molecule among the Gram-negative bacteria, which is a 325-amino acid protein, out of which 177 amino acids at the N-terminal portion are shown to cross the membrane eight times in antiparallel β -strands with four relatively large and hydrophilic surface-exposed loops and short periplasmic turns (24–27). The remaining C-terminal region sits in the periplasmic area of the bacteria. The function of OmpA is thought to contribute to the structural integrity of the outer membrane along with murein lipoprotein and peptidoglycan-associated lipoprotein (28–31). OmpA also serves as a receptor of colicin and several phages, which is required in F-conjugation (32, 33). OmpA-like proteins are present in all 17 genera of Gram-negative bacteria, and a comparison of five OmpA homologues from five closely

* This work was supported, in whole or in part, by National Institutes of Health Grants AI40567 and NS73115 (to N. V. P.). This work was also supported by Saban Research Institute research career development fellowship (to R. M.).

[5] The on-line version of this article (available at <http://www.jbc.org>) contains supplemental Figs. 1–4.

¹ To whom correspondence should be addressed: Division of Infectious Diseases, MS 51, Childrens Hospital Los Angeles, 4650 Sunset Blvd., Los Angeles, CA 90027. Tel.: 323-361-5465; Fax: 323-361-2867; E-mail: pnemani@chla.usc.edu.

² The abbreviations used are: HBMEC, human brain microvascular endothelial cell; DC, dendritic cells; PMN, polymorphonuclear lymphocyte; CFU, colony-forming unit; HBSS, Hanks' balanced salt solution.

OmpA Domains Involved in the Onset of *E. coli* K1 Meningitis

related genera indicated that the β -sheet residues of the N termini are highly conserved, although the extracellular loops have relatively large variations (34). Koebnik (35, 36) has shown that the extracellular loops of OmpA can be deleted without affecting the assembly of the β -barrel structure. However, it is strongly believed that deletion of portions of extracellular loops affects the function of OmpA (31), although the roles of various loops of OmpA in the pathogenesis of *E. coli* K1 have not been examined to date. We have generated a variety of OmpA mutants by changing three or four amino acids at a time to alanines and demonstrated that some regions of loops 1, 2, and 4 of OmpA are critical for the invasion of *E. coli* K1 in HBMEC (37). Here, we further analyze the effects of mutations in OmpA-mediated interaction with C4bp, various immune cells, and the occurrence of meningitis in a newborn mouse model of meningitis.

EXPERIMENTAL PROCEDURES

Generation of OmpA Mutants of *E. coli* K1—*E. coli* K1 strain E44 (OmpA⁺) is a rifampin-resistant mutant of the clinical isolate RS218, and E98 (OmpA⁻) is an *ompA*-deletion mutant of E44 (13). Various mutations in OmpA were generated as described previously using the plasmid pKE325 (low copy number), which is a pACYC derivative (pK194) containing the entire *ompA* gene with its own promoter (37). Briefly, primer pairs containing the desired mutations were synthesized and cartridge-purified. PCR for the plasmid mutation was carried out using *PfuTurbo* DNA polymerase and pKE325 as the template. A faint band was visualized on agarose gel if the amplification succeeded. DNA was then digested with DpnI and transformed into *E. coli* DH5 α followed by selecting for kanamycin resistance. Plasmids were isolated, and the mutation was verified by sequencing. The correct plasmids were introduced into the Δ *ompA* strain E98. The expression of OmpA on each mutant strain of *E. coli* was determined by flow cytometry. *E. coli* strains grown overnight were centrifuged and washed twice with Hanks' balanced salt solution (HBSS) at room temperature. The bacteria were resuspended in HBSS and adjusted to 1×10^9 CFU/ml. The bacterial suspension was incubated with anti-OmpA antibody (1:10,000 dilution) at 37 °C for 1 h, and the unbound antibody was removed by centrifugation, and the bacteria were washed three times with PBS. The bacterial pellets were then incubated with FITC-conjugated secondary antibody for 30 min at room temperature, washed, and resuspended in PBS. Flow cytometry analysis was carried out on a flow cytometer (BD Biosciences) using CellQuest software, and $\sim 10,000$ events were recorded.

Isolation of Outer Membrane Proteins and Western Blotting—Outer membrane proteins from *E. coli* K1 were isolated as described previously (38). Various strains of *E. coli* K1 mutants were grown overnight in LB broth containing 100 μ g of rifampin or 50 μ g of kanamycin per ml. The bacteria were collected by centrifugation and washed three times with TE buffer (20 mM Tris, 10 mM EDTA, pH 7.4). The pellet was then resuspended in 1 ml of TE buffer, sonicated three times for a minute each time, and centrifuged at $6000 \times g$ for 10 min at 4 °C. The pellet was discarded, and the supernatant

was subjected to ultracentrifugation at $45,000 \times g$ for 45 min at 4 °C. The pellet was resuspended in 1% sodium lauryl sarcosinate in TE buffer and incubated at 37 °C for 2 h to completely digest the inner membrane. The solution was then subjected to ultracentrifugation at $45,000 \times g$ for 45 min at 4 °C, and the pellet was suspended in 20 μ l of 1% SDS in TE buffer. 10 μ g of outer membrane preparations were separated on 10% SDS-PAGE and subjected to Western blotting with anti-OmpA antibody (38).

Dot Blot Analysis of *S-Fimbriae* Expression—Bacterial lysates (50 μ g) prepared from 10^7 CFU/ml of various *E. coli* K1 mutants were spotted onto nitrocellulose membrane and allowed to dry for 15 min. The blot was blocked with 5% milk in PBS, then probed with anti-*S-fimbriae* antibody (1:1000 dilution), and incubated for 90 min at room temperature. The blot was washed three times with PBS/Tween 20 (PBST) and incubated with HRP-conjugated anti-mouse secondary antibody for 1 h at room temperature. After five washes with PBST, the blot was developed using SuperSignal West Pico chemiluminescent substrate (Pierce) (39). The blot was scanned, and the densities of the dots were quantified using ImageJ software (National Institutes of Health). A score of +++ means that the density was similar to that of WT *E. coli* K1.

Growth Pattern of Various *E. coli* K1 Strains—The growth pattern of the OmpA⁺, OmpA⁻, and the loop mutants of *E. coli* was analyzed using the spectrophotometric turbidity method at 600 nm (A_{600}). 1% of overnight cultures of the strains were subcultured in 20 ml of LB broth, and absorbance was measured as the zero-hour reading. The cultures were then incubated at 37 °C with constant shaking at 220 rpm, and 1 ml of the respective cultures was taken at every hour, and the absorbance was measured again.

Yeast Aggregation Assay—To analyze type 1 fimbriae expression, the mutant strains were subjected to yeast aggregation assay as described previously (40). In short, the mutants were cultured overnight, and their absorbance was adjusted to 0.4 at 530 nm using sterile PBS. 20 μ l of each of the cultures was mixed with 20 μ l of a 5 mg/ml suspension of commercial grade yeast in sterile PBS on a clean glass slide. Scoring for the agglutination was made based on visual observation of agglutination. A score of ++++ represents strong agglutination within 10 s of mixing. Subsequent scoring was based on additional 10-s time periods.

Total Polysaccharide Content Determination—Total keto-deoxyoctulosonate estimation was performed as described previously (17). Briefly, 10^{10} CFU of bacteria were harvested, pelleted, washed once in PBS, and resuspended in 5 ml of cold PBS. Twenty microliters were removed for quantitative estimation of the bacteria, and the remaining suspension was sonicated continuously at 50% power for 4 min on ice. Following sonication, 200 μ l was mixed with 0.1 ml of the periodate solution (0.2 M in 9 M phosphoric acid). The tubes were agitated and allowed to stand at room temperature for 20 min. Then 1 ml of sodium arsenite solution (10% in a solution of 0.5 M sodium sulfate, 0.1 N H₂SO₄) was added and mixed until a yellow-brown color appeared followed by the addition of 3 ml of thiobarbituric acid (0.6% in 0.5 M sodium sulfate).

The tubes were shaken and heated vigorously in a boiling water bath for 15 min. 1 ml of this solution was transferred to another tube, which contained 1 ml of cyclohexanone. The tube was shaken twice and then centrifuged for 3 min at $1000 \times g$. The clear upper red-colored cyclo-hexanone phase was collected, and the absorbance was measured at 549 nm. The molecular extinction coefficient used was 57,000. The amount of keto-deoxyoctulosonate present in a given sample is determined from the following equation: $V \times A_{549}/57 = 4.3 \times A_{549}/57 = 0.075 \times A_{549}$, where V is the final volume of the test solution.

Serum Survival Assays—The bacterial suspensions (10^6 CFU/ml) were incubated with freshly prepared serum diluted to 40% in gelatin/veronal buffer (Sigma) (17). Aliquots of 10 μ l were removed at various times and serially diluted in saline, and dilutions were plated on sheep blood agar. The plates were incubated at 37 °C overnight; the colonies were counted, and percent survival was calculated and compared with the survival of wild type *E. coli* K1.

C4bp Binding Assays—The binding of C4bp to bacteria was examined by flow cytometry (17). *E. coli* K1 strains grown overnight were centrifuged and washed twice with HBSS at room temperature. The bacteria were resuspended in HBSS and adjusted to 1×10^9 cells/ml. The bacterial suspension was incubated with 200 nM purified C4bp at 37 °C for 1 h, and the unbound C4bp was removed by centrifugation, and the bacteria were washed with PBS three times. The bacteria were then incubated with C4bp antibody (1:1000 dilution) (Calbiochem) at room temperature for 1 h followed by three washings with PBS. The bacterial pellets were then incubated with FITC-conjugated secondary antibodies for 30 min at room temperature, washed, and resuspended in PBS. Flow cytometry analysis was carried out on a flow cytometer (BD Biosciences) as described above.

Determination of *E. coli* K1 Entry and Survival in DCs, Polymorphonuclear Leukocytes (PMNs), and Peritoneal Macrophages—Monocyte-derived myeloid DCs were isolated from the blood of human volunteers as described previously (19). Mouse DCs were obtained by differentiating bone marrow cells isolated from the femurs and tibias of mice (23). PMNs were isolated from the peripheral blood of the human volunteers and mice as described previously (21, 41, 42). IRB of Children's Hospital Los Angeles approved the blood withdrawal protocol from human volunteers. Macrophages were isolated from the peritoneal cavity of mice as described earlier (22, 43). Total bacteria entered and the intracellular bacteria in neutrophils, DCs, and macrophages were determined as described previously (19, 21–23). Respective cells were incubated with bacteria at a multiplicity of infection of 10 (cell to bacteria ratio, 1:10) at 37 °C for 2, 4, and 6 h. At different post-infection times, the co-cultures were centrifuged at a low speed ($700 \times g$); aliquots from the supernatants were diluted and plated on blood agar. The number of bacteria present in the supernatants was subtracted from the total number of bacteria added to co-cultures to obtain the number of bacteria entering the phagocytes. To assess the intracellular bacteria, the co-cultures were centrifuged at a low speed to pellet the cells; gentamicin was added at a final concentration of 100 μ g

ml⁻¹ to the pellet, and the cells were incubated for an additional 60 min at 37 °C. The co-cultures were washed three times; the cells were lysed with 0.5% Triton X-100, and the released intracellular bacteria were enumerated by plating the dilutions on blood agar.

Newborn Mouse Model of Meningitis—The animal studies were approved by the Institutional Animal Care and Use Committee (IACUC) of the Saban Research Institute at Children's Hospital Los Angeles and followed National Institutes of Health guidelines for the performance of animal experiments. Three-day-old mice were infected intranasally with 10^3 CFU of bacteria in 10 μ l of saline (21, 22). Control mice received pyrogen-free saline through the same route. At different times post-infection, blood was collected from the tail or facial vein and plated on antibiotic-containing LB agar. The occurrence of meningitis was assessed by culturing 5 μ l of cerebrospinal fluid obtained by cisternal puncture, without traumatic tap, into LB broth containing antibiotics (21, 22). Mice were perfused intracardially with saline to remove blood as well as contaminating intravascular leukocytes. Various tissues were aseptically harvested and homogenized in sterile PBS, and the bacterial counts were determined by plating 10-fold serial dilutions on rifampicin- or kanamycin-containing LB agar.

Determination of the Blood-Brain Barrier Leakage—Newborn mice infected with *E. coli* K1 were given an intraperitoneal injection of 2% Evans blue dye at 68 h post-infection or 20 h in the case of mice infected with loop 4 mutants. After 4 h, the animals were anesthetized with Nembutal and transcardially perfused with PBS until colorless perfusion fluid was obtained from the right atrium. The brains were harvested, weighed, homogenized in PBS, and centrifuged to collect the supernatants. Evans blue intensity in the supernatants was determined by a microplate reader at 550 nm. Calculations were based on the external standards dissolved in PBS. The amount of Evans blue was quantified as micrograms/mg protein (22).

Histopathological Analysis—Half of the brain was fixed in 10% buffered formalin, routinely processed, and embedded in paraffin. 4–5- μ m sections were cut using a Leica microtome and stained with hematoxylin and eosin (H&E) (21, 22). The slides were read by a neuropathologist in a blinded fashion.

Quantitative Assessment and Phenotypic Characterization of Brain Leukocytes—Characterization of leukocytes derived from brains of newborn mice was performed using flow cytometry, as described previously, using various antibodies obtained from eBiosciences (San Diego) (21). Murine microglia and macrophages were identified by staining with anti-CD45 (LAC)-biotin and anti-F4/80-FITC, respectively, followed by avidin-PE/Cy5. Inflammatory leukocytes recruited to the brain are CD45^{high} F4/80⁻; macrophages are CD45^{high} F4/80⁺, and microglia are CD45^{low} F4/80⁺. CD4⁺ and CD8⁺ T lymphocytes were stained with rat anti-mouse CD4 followed by goat anti-rat phycoerythrin and anti-CD8 FITC, respectively. B lymphocytes were detected by staining with anti-CD45R (B220)-FITC and anti-CD45 (LCA)-biotin followed by avidin-phycoerythrin/Cy5. Granulocytes were

OmpA Domains Involved in the Onset of *E. coli* K1 Meningitis

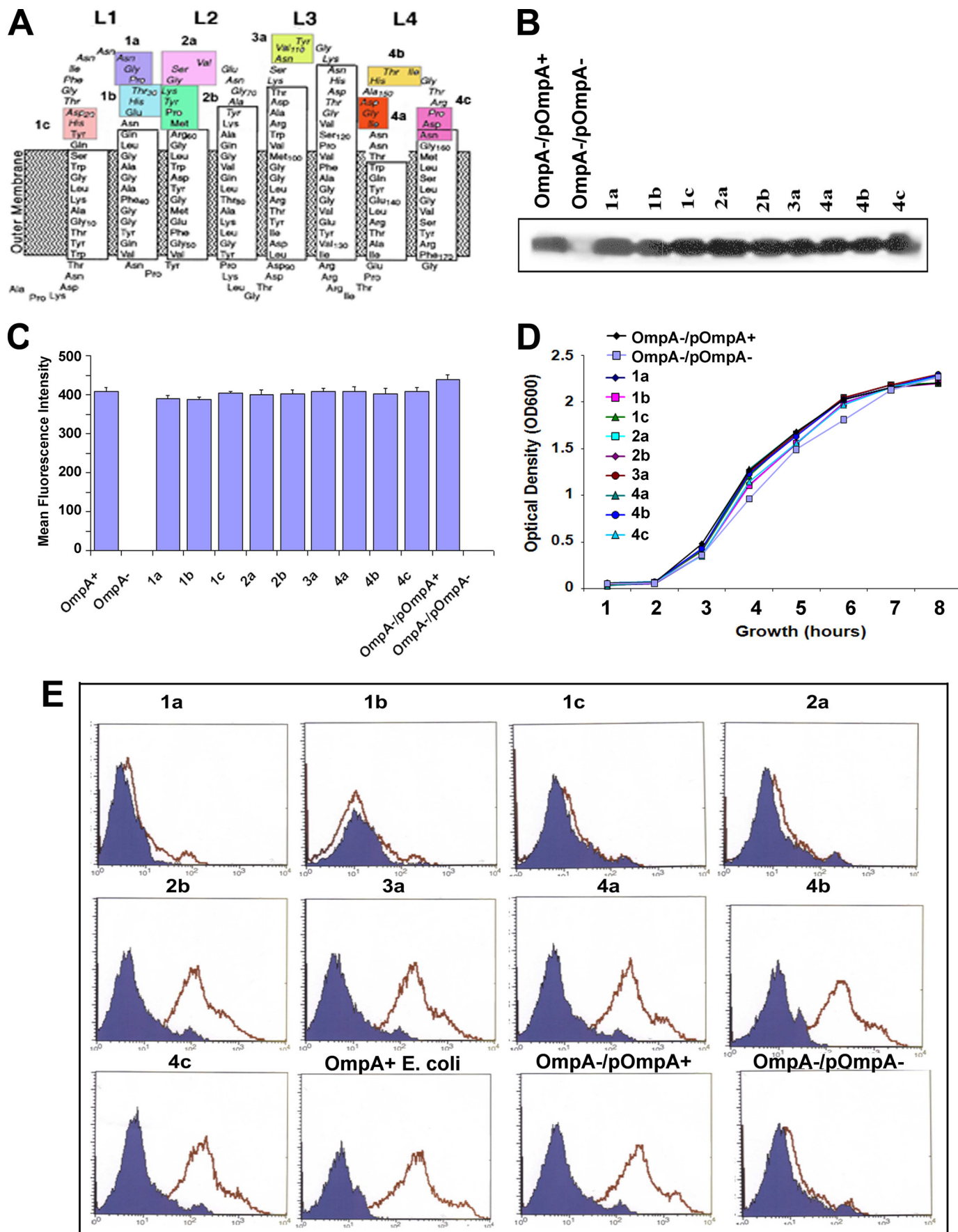


TABLE 1
Phenotypic characteristics of various *E. coli* K1 strains

Strains	Serum susceptibility (50% inhibition of bacteria) ^a	S-fimbriae expression	Type 1 fimbriae expression	α -Hemolysin on blood agar	Total keto-deoxyoctulosonate (LPS and capsule) in micrograms/10 ⁸ cells
1a	+	+	+++	+	13.85 \pm 0.84
1b	+++	+	++++	+	13.45 \pm 0.84
1c	+++	+	++++	+	12.52 \pm 0.73
2a	+	+	+++	+	13.39 \pm 1.25
2b	–	+	++++	+	12.49 \pm 0.007
3a	–	+	++++	+	16.06 \pm 0.34
4a	+	+	++++	+	14.88 \pm 0.84
4b	+	+	+++	+	14.28 \pm 0.056
4c	+	+	++++	+	10.12 \pm 0.84
OmpA [–] /pOmpA ⁺	–	+	++++	+	13.90 \pm 0.85
OmpA [–] /pOmpA [–]	+++	+	++	+	12.82 \pm 0.42

^a +++ indicates bacterial inhibition was at 0–15 min, and + indicates at 30–60 min.

stained with anti-Ly6-G (GR-1) followed by goat anti-rat phycoerythrin and F4/80 FITC. Granulocytes were defined as Ly6-G⁺ F4/80. Control staining included incubation of brain-derived leukocytes with unlabeled or fluorochrome-labeled isotype-matched control antibodies. Flow cytometry was performed as described above.

Cytokine Determination—The levels of cytokines in the serum and brain tissue homogenates of infected mice were measured using ELISA kits according to the manufacturer's instructions (BIOSOURCE).

Statistical Analysis—Analysis of variance, Fischer test, χ^2 test, and paired Student's *t* test were applied. A value of *p* < 0.05 was considered significant.

RESULTS

Changing Three or Four Amino Acids to Alanines in the Extracellular Loops Had No Effect on General Phenotypic Characteristics of *E. coli* K1 and the Interaction with C4bp—In view of dissecting the roles of various domains of OmpA in the pathogenesis of *E. coli* K1 meningitis, we have generated several strains of *E. coli* K1 expressing OmpA in which three or four amino acids in various extracellular loops have been changed to alanines, and a diagram showing the location of mutations is depicted in Fig. 1A. Computer modeling studies of mutant OmpA in comparison with wild type OmpA showed no significant differences in the structure (37). The plasmids containing mutations were transformed into E98, which is an OmpA[–] *E. coli* K1. The expression of OmpA was equal in all these strains as analyzed by Western blotting of the outer membrane proteins of various mutants with an anti-OmpA antibody (Fig. 1B). In addition, the expression of OmpA on the surface of *E. coli* K1 also did not differ significantly as determined by flow cytometry (Fig. 1C). The growth curves of mutant *E. coli* K1 exhibited no differences; however, bacteria that lack OmpA expression grew slightly slower compared with OmpA⁺ *E. coli* K1 (Fig. 1D). In addition, the levels of S-

fimbriae and total polysaccharide content were also determined by dot blot analysis and thiobarbituric acid assay, respectively. As shown in Table 1, no significant differences were observed in the amounts of these two components produced among various strains. Similarly, the production of hemolysin was also unchanged in different mutants as determined by the halo reaction on blood agar plates. It was previously shown that the lack of OmpA expression suppresses the level of type 1 fimbriation, which might contribute partially to the binding of *E. coli* K1 to endothelial cells (44). Analysis of type 1 fimbriation indicated that, indeed, OmpA[–] *E. coli* K1 expressed lower type 1 fimbriae as determined by yeast agglutination assay (34). OmpA⁺ *E. coli* K1 and other bacteria expressing mutant OmpA showed no significant differences in the expression of type 1 fimbriae (Table 1). These results indicate that the expression of OmpA or other surface structures did not vary significantly in *E. coli* K1 mutants when compared with WT *E. coli* K1.

As we have previously shown that OmpA expression is critical for the serum survival because of its binding to C4b-binding protein (C4bp), all the *E. coli* K1 mutants were examined for their ability to evade serum bactericidal activity (16, 17). OmpA⁺ *E. coli* K1 survived to an extent of 60% by 2 h postincubation with 40–60% serum, whereas OmpA[–] *E. coli* K1 strain was killed by 90% after 1 h. *E. coli* mutants 1b and 1c cells were killed completely within 15 min by serum, whereas mutants 1a, 2a, 4a, 4b, and 4c were killed by 60% between 30 and 60 min incubation with serum. The survival rates of 2b and 3a mirrored that of OmpA⁺ *E. coli* K1. Binding analysis of C4bp to various mutants of *E. coli* K1 by flow cytometry revealed that 1a, 1b, 1c, and 2a were unable to bind C4bp (Fig. 1E). However, other mutants had retained the binding capacity similar to that of OmpA⁺ *E. coli* K1. These results suggest that regions in loops 1, 2, and 4 of OmpA are involved in resisting serum bactericidal activity via increased binding to C4bp.

FIGURE 1. Characterization of *E. coli* K1 strains expressing various mutant OmpAs. Schematic showing two-dimensional structure of OmpA in which regions in the extracellular loops have been mutated are highlighted (A). Equal amounts of outer membrane proteins (10 μ g) were separated by SDS-PAGE and subjected to Western blotting with anti-OmpA antibody (B). *E. coli* K1 strains were incubated with anti-OmpA antibody for 1 h, washed, and further incubated with FITC-coupled secondary antibody. After thorough washing, the bacteria were subjected to flow cytometry. Mean fluorescence intensities after subtracting respective isotype-matched antibody values are graphed (C). Various *E. coli* K1 strains were examined for their growth profile as described under "Experimental Procedures" (D). In addition, binding of *E. coli* K1 mutants to C4bp was determined by flow cytometry. The solid area represents respective isotype control (E). The data represent mean values \pm S.D. The results are representative of six independent experiments carried out in triplicate.

OmpA Domains Involved in the Onset of *E. coli* K1 Meningitis

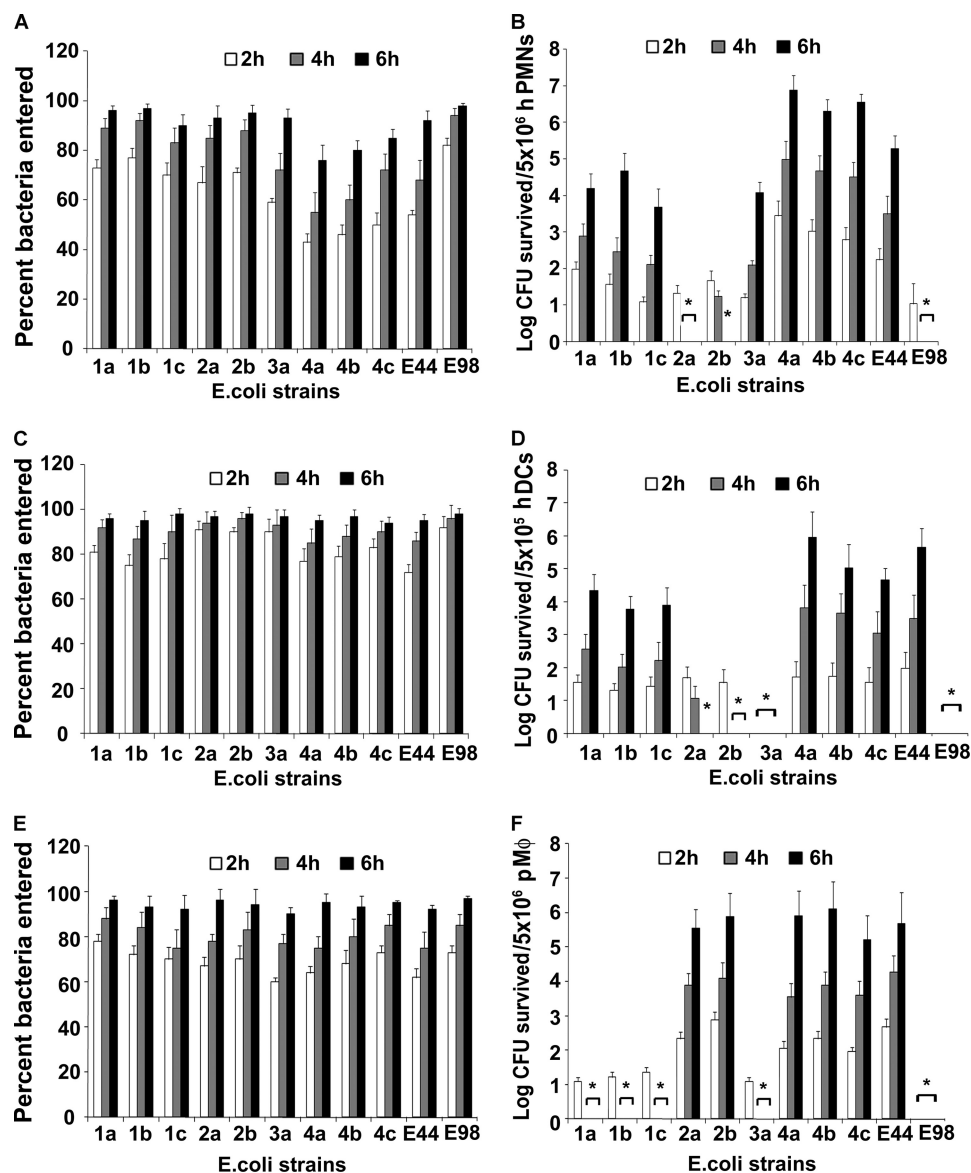


FIGURE 2. Various loop regions of OmpA are necessary for the survival of *E. coli* K1 in different immune cells. The entry and survival of *E. coli* K1 expressing mutant OmpA in PMNs (A and B), DCs (C and D), and macrophages (E and F) was determined as described under "Experimental Procedures." The results are expressed as means \pm S.D. and representative of four independent experiments performed in triplicate. *, $p < 0.01$ versus OmpA⁺ *E. coli* K1 (E44) by two-tailed Student's *t* test.

Different Loop Regions of OmpA Are Involved in the Survival of E. coli K1 Inside Immune Cells—Because PMNs are the first line of defense against invading pathogens, we examined the effects of loop mutations in OmpA on the interaction of *E. coli* K1 with human PMNs. Interestingly, we observed that there were no significant differences in the entry of *E. coli* K1 mutants in PMNs (Fig. 2A). However, *E. coli* mutants 2a and 2b could not survive and multiply inside PMNs comparable with OmpA[−] *E. coli*, whereas 4a, 4b, and 4c survived similar to that of OmpA⁺ *E. coli* K1 (Fig. 2B). Bacteria with mutations in loops 1 and 3 of OmpA, however, exhibited slightly diminished multiplication up to 6 h post-infection. Similar results were also observed in mouse PMNs (supplemental Fig. S1, A and B). Our previous studies have demonstrated that OmpA⁺ *E. coli* K1 suppresses the production of pro-inflammatory cytokines and enhances the production of anti-inflam-

matory cytokines in dendritic cells (DCs), the most potent antigen-presenting cells, for which OmpA expression is necessary (19). Therefore, we determined which regions of OmpA are required to enter and survive inside human DCs. No statistically significant differences were observed in the entry of OmpA mutant strains in DCs compared with wild type OmpA⁺ *E. coli* K1 (Fig. 2C). However, mutations in loop 2 and loop 3 significantly prevented their survival in DCs (Fig. 2D). In contrast, mutations in loop 4 did not alter the survival, whereas mutations in loop 1 showed intermediate survival up to 6 h post-infection as seen in PMNs. A similar pattern of phagocytosis was also observed in mouse bone marrow-derived DCs (supplemental Fig. S1, C and D). Furthermore, OmpA⁺ *E. coli* K1 has been shown to persist and proliferate inside macrophages. Therefore, we next examined the phagocytosis of OmpA mutant strains by mouse peritoneal macrophages. All the mutant

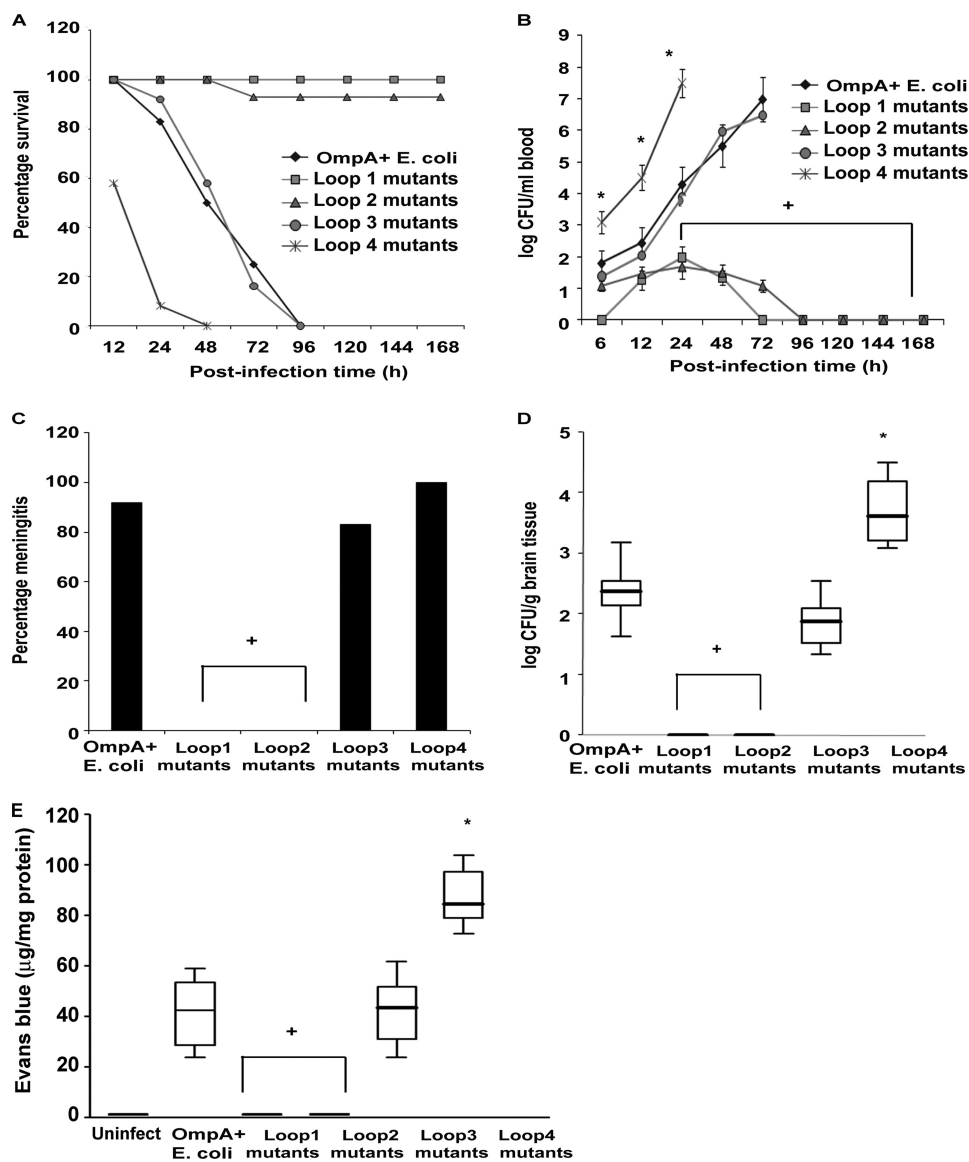


FIGURE 3. Mutations in the extracellular loops of OmpA affect the ability of *E. coli* K1 to cause meningitis. Newborn mice at day 3 were infected intranasally with 10^3 CFU of *E. coli* K1, and survival was monitored over time. The number of animals survived at each time point is indicated (A). Blood was collected at various post-infection time intervals; dilutions were made and plated on antibiotic containing agar (B). Cerebrospinal fluid samples were obtained from the same animals and directly inoculated into LB broth containing antibiotics (C). *E. coli* K1 strains transformed with plasmids containing OmpA in which loop 4 mutations were incorporated showed higher brain bacterial titers compared with other strains (D). The blood-brain barrier permeability was assessed using the Evans blue extravasation technique as described under "Experimental Procedures" (E). The results were obtained from five independent experiments. Data represent means \pm S.D. *, $p < 0.05$, and +, $p < 0.01$ versus OmpA⁺ *E. coli* K1 by two-tailed Student's *t* test.

strains of *E. coli* K1 were phagocytosed in similar numbers by macrophages (Fig. 2E). Of note, mutants 2a, 2b, 4a, 4b, and 4c exhibited survival ability in mouse peritoneal macrophages similar to OmpA⁺ *E. coli* K1. The number of intracellular bacteria recovered from macrophages increased by 6 h compared with 2 h post-infection, the same as that of PMNs and DCs, indicating proliferation of bacteria inside macrophages (Fig. 2F). In contrast, mutants 1a, 1b, 1c, 3a, and OmpA⁻ *E. coli* K1 were efficiently killed by macrophages. Studies with mouse bone marrow-derived macrophages showed similar results (supplemental Fig. S1, E and F). These data suggest that OmpA regions in loop 2 are critical to interact with PMNs, whereas loops 2 (amino acids) and 3 domains are necessary for interaction with DCs. In contrast, regions in loops 1 and 3 are important for survival inside macrophages.

*Mutations in Loops 1 and 2 of OmpA Render E. coli K1 Inefficient at Causing Meningitis, whereas Loop 4 Mutants Show Increased Virulence in a Mouse Model of Neonatal Meningitis—*Next, we sought to determine the effects of OmpA mutations on the ability of *E. coli* K1 to cause meningitis in a mouse model. The animal experiments were performed with all the mutants independently, and for the sake of presenting data, they were divided into four groups as they yielded similar results. Approximately 90% of the animals infected with loop 4 mutants became moribund within 24 h post-infection, whereas 100% of mice infected with loop 3 mutants and OmpA⁺ *E. coli* K1 were in a similar state by 96 h post-infection (12/145 pups, Fig. 3A). Because of ethical reasons, the animals in moribund stage were sacrificed. However, animals infected with loop 1 and loop 2 mutants showed substantially

OmpA Domains Involved in the Onset of *E. coli* K1 Meningitis

better survival even at higher doses of infection and were finally sacrificed at 168 h post-infection (Fig. 3A). Infection with loop 4 mutants showed a sharp increase in bacteremia within 24 h of infection, although loop 3 mutants and OmpA⁺ *E. coli* K1 reached similar levels by 72 h (Fig. 3B). In contrast, loop 1 mutants entered the blood slowly with a peak bacteremia at 24 h post-infection showing a 2.00 log₁₀ CFU and were subsequently cleared from circulation by 72 h post-infection. However, loop 2 mutants entered the blood by 6 h post-infection and were cleared from circulation by 96 h. In agreement with the bacteremia levels, 100% of the cerebrospinal fluid cultures were positive in loop 4 mutant infected mice, whereas none of the cerebrospinal fluid cultures were positive in loop 1 and loop 2 infected animals (Fig. 3C). The brain bacterial titers were significantly higher in loop 4 mutant infected mice compared with OmpA⁺ *E. coli* K1 or loop 3 mutant infected animals (Fig. 3D). In contrast, brain cultures were sterile in mice infected with loop 1 and loop 2 mutants. In agreement with these findings, brain tissue damage markers lactate dehydrogenase and malonaldehyde were significantly increased, whereas glutathione was decreased indicating oxidative stress in loop 4 mutant infected mice compared with animals infected with OmpA⁺ *E. coli* K1 or loop 3 mutants (supplemental Fig. S2, A–C). Because bacterial multiplication in tissues to reach a high level of bacteremia is important for crossing the blood-brain barrier, we determined the bacterial load in other organs to examine whether the bacteria were trapped in these organs. High numbers of loop 4, loop 3, and OmpA⁺ *E. coli* K1 were recovered from the intestine, liver, lung, spleen, and kidneys of infected mice at 24 h post-infection (supplemental Fig. S3, A–E). In contrast, very low numbers of bacteria were present in these organs in animals infected with loop 1 and loop 2 mutants. In agreement with these results, animals infected with loop 4 mutants showed greater disruption of the blood-brain barrier compared with mice infected with loop 3 mutants and OmpA⁺ *E. coli* K1 as demonstrated by Evans blue extravasation method (Fig. 3E). Interestingly, no disruption of the blood-brain barrier was observed in loop 1 and loop 2 mutant infected animals. These results suggest that regions in loops 1 and 2 are responsible for surviving in tissues and/or blood to reach high grade bacteremia, a prerequisite for the onset of meningitis.

Mutations in Loop 4 Cause Exaggerated Pathology in the Brains of Infected Mice—Because loop 4 mutants infected mice succumbed earlier than wild type *E. coli* K1-infected animals, we speculated that loss of epitopes in loop 4 might contribute to lethal immune response by surviving better in the animals. Therefore, we first examined the number and types of cells recruited to the brains of mice infected with various mutant strains of *E. coli* K1. Interestingly, loop 1 and 2 mutant strains, which were cleared from the host faster than the wild type *E. coli*, demonstrated more numbers of CD4⁺ and CD8⁺ T cells in brains, indicating that cellular immunity may be important for the clearance (Fig. 4, A–F). In contrast, loop 4 mutants, showing higher virulence, recruited more microglia, B cells, macrophages, and granulocytes. Similarly, loop 4 mutants upon infection elicited higher production of

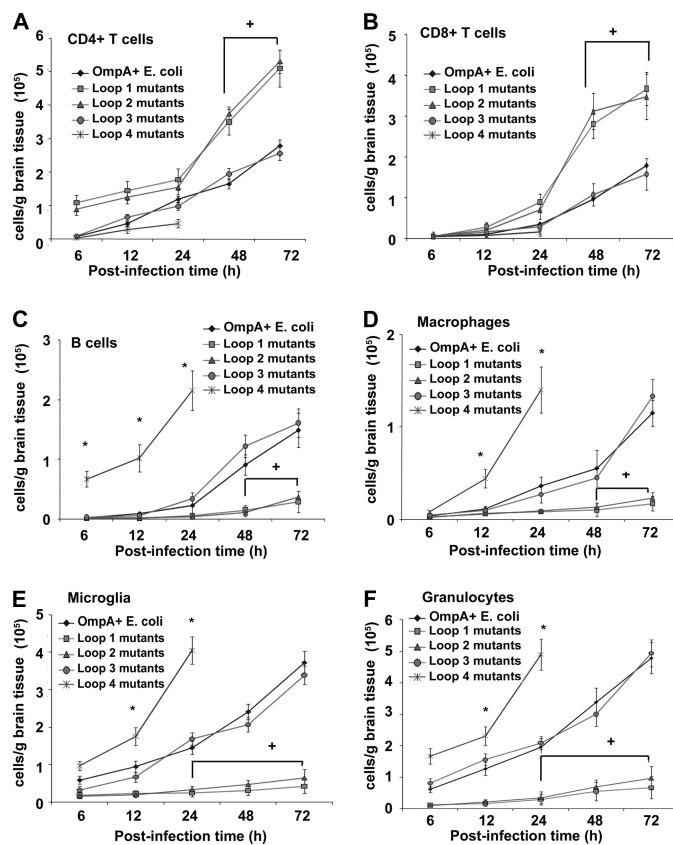


FIGURE 4. Recruitment of various types of cells in mice infected with *E. coli* K1. The influx of CD4⁺ (A) and CD8⁺ (B) T cells as well as B cells (C), macrophages (D), microglia (E), and granulocytes (F) into the brains of infected mice was determined by flow cytometry. Mice infected with OmpA⁺ *E. coli* K1, loop 4, and loop 3 mutants showed more recruitment of B cells, macrophages, microglia, and granulocytes, and there was more influx of CD4⁺ and CD8⁺ T cells in loop 1 and loop 2 infected animals. The data are representative of five independent experiments with at least 10 animals per group at each time point. Data represent means \pm S.D. *, $p < 0.05$, and +, $p < 0.01$ versus OmpA⁺ *E. coli* K1 by two-tailed Student's *t* test.

TNF- α , IL-1 β , IL-6, and IL-12 in blood compared with loop 3 mutants or OmpA⁺ *E. coli* K1 (Fig. 5, A–D). In contrast, loop 1 and loop 2 mutants showed significantly lower production of these cytokines. The entry of bacteria into the brain was accompanied by the activation of immune responses leading to generation of high levels of inflammatory cytokines, which constitutes the first line of self-defense against bacterial infections. However, exaggerated production of cytokines is a major cause of complications associated with meningitis and septic death. Therefore, we examined cytokine levels in brain tissues of mice infected with *E. coli* K1. We observed that levels of TNF- α , IL-1 β , IL-6, and IL-12 were significantly high in the brains of mice infected with loop 4 mutants compared with animals infected with loop 3 mutants or OmpA⁺ *E. coli* K1 (supplemental Fig. S4, A–D). Next, we determined the extent of brain damage in infected mice. Of note, loop 4 mutants caused more severe brain damage compared with OmpA⁺ *E. coli* K1-infected pups. Histopathology of brains from mice infected with loop 4 mutants displayed meningeal thickening and hemorrhage (Fig. 6). Severe leukocyte infiltration was observed in the cortex and white matter. Neurons exhibited pyknotic nuclei spanning entire regions of the den-

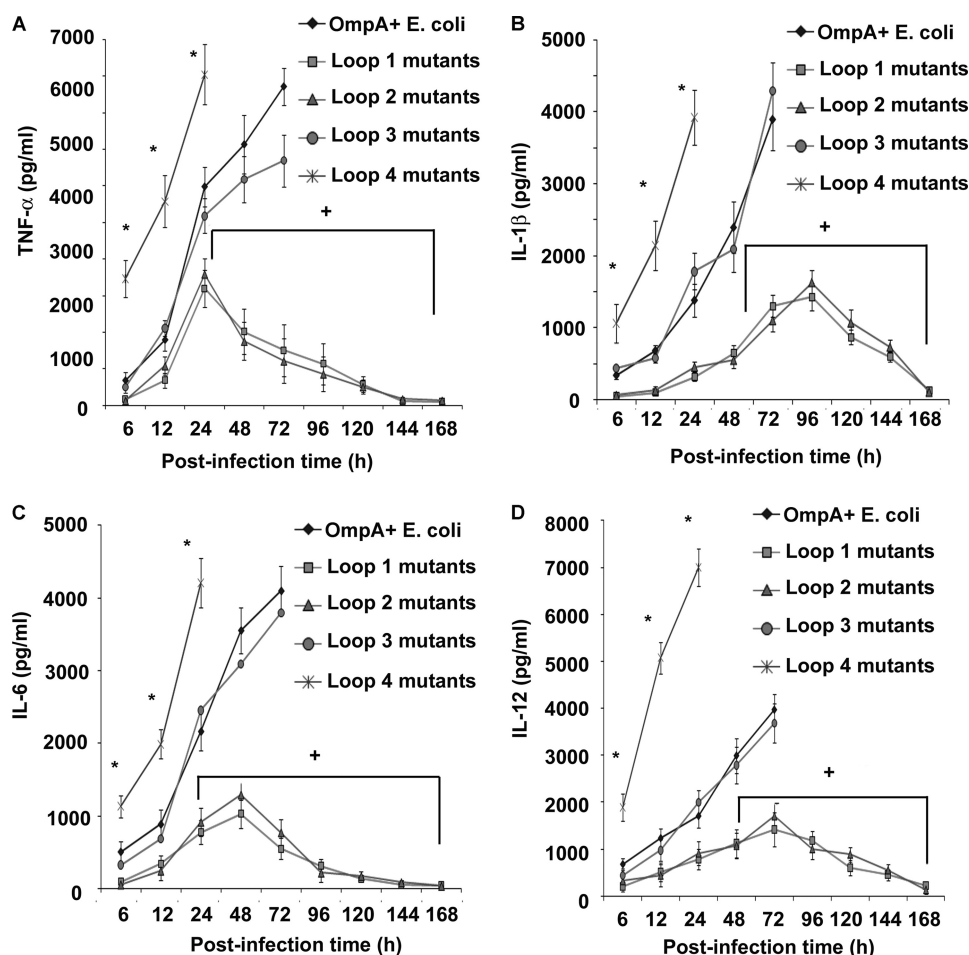


FIGURE 5. Serum cytokine levels in *E. coli* K1-infected mice. Blood was collected from infected mice, and the levels of TNF- α (A), IL-1 β (B), IL-6 (C), and IL-12 (D) production were determined by ELISA. Loop 4 mutants induced elevated production of these pro-inflammatory cytokines compared with those of other strains. The results were obtained from five independent experiments with at least 10 animals per group at each time point. Data represent mean values \pm S.D. *, $p < 0.05$, and +, $p < 0.01$ versus OmpA⁺ *E. coli* K1 by two-tailed Student's *t* test.

tate gyrus in the hippocampus of these mice. Severe hemorrhagic lesions were seen in the brain parenchyma of mice infected with loop 4 mutant strains of *E. coli* K1. All these changes were present but less pronounced in OmpA⁺ *E. coli* K1 or loop 3 mutant infected mice. However, animals infected with 1a, 1b, 1c, 2a, and 2b strains showed no brain damage similar to control uninfected animals. These results indicate that the pathophysiological manifestation of brain damage in animals infected with loop 4 mutants may be due to the entry of a greater number of bacteria, which in turn induced an exacerbated immune response.

DISCUSSION

In Gram-negative bacteria, the function of OmpA is thought to contribute to the structural integrity of the outer membrane (28–30). Recently, Power *et al.* (45) had identified two alleles of *ompA*, *ompA1* and *ompA2*. The nucleotide sequence differences of these alleles translate into several amino acid changes in the second and third extracellular loops. Our previous studies have shown that OmpA expression is very critical for the invasion of HBMEC by binding to Ecgp96 and that OmpA⁻ *E. coli* K1 strains were 25–50-fold less invasive than the parental strain (13). Furthermore, we also demonstrated that two synthetic peptides corresponding to the

sequences of loop 1 and loop 2 of OmpA significantly prevented the invasion of *E. coli* in HBMEC, albeit at high concentrations (15). Of note, the peptide sequence mimicking the region of loop 2 maps to the areas of OmpA that differ between *ompA1* and *ompA2* alleles (45). This indicates that specific subsets of OmpA exist that may be more or less invasive depending on the loop 2 amino acid sequence. The role of OmpA is not solely restricted to meningitic *E. coli* K1 binding to HBMEC. Enterohemorrhagic *E. coli* of serotype O157:H7 utilizes OmpA in adhering to HeLa epithelial cells and Caco-2 colonic epithelial cells (46). OmpA also appears to be critical in adherence to plant surfaces, as an *ompA* mutant of *E. coli* O157 did not colonize alfalfa bean sprouts (47). In addition, OmpA, together with the Hek protein, has been shown to be critical for the invasion of colonic epithelial cells by meningitic *E. coli* (48). We have further demonstrated that OmpA expression is necessary for the interaction of *E. coli* K1 with neutrophils, dendritic cells, macrophages, and complement protein C4bp (16–20). Nonetheless, no studies have been attempted to map out the regions of OmpA extracellular loops that interact with various host elements. Therefore, we sought to define the regions of *E. coli* K1 OmpA that

OmpA Domains Involved in the Onset of *E. coli* K1 Meningitis

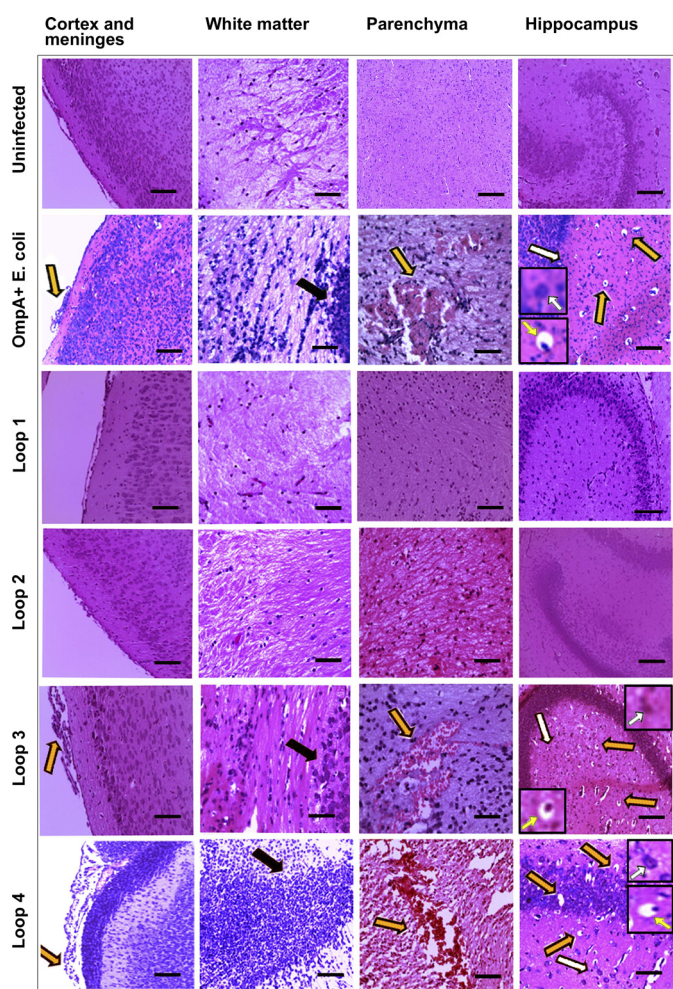


FIGURE 6. Mutations in loop 4 of OmpA lead to exaggerated brain damage in a mouse model of neonatal meningitis. Brains were harvested from *E. coli* K1-infected mice and subjected to H&E staining. Neutrophil infiltration (yellow arrow) in the cortex and meninges in brains of mice infected with loop 3 mutants or OmpA⁺ *E. coli* K1 was observed. These animals also showed infiltration of inflammatory cells evident in white matter (black arrow) and acute hemorrhage (yellow arrow) in the brain parenchyma. Hippocampus showed apoptosis of neurons (yellow arrow and inset) and inflammation (white arrow and inset). All the pathological changes in these brains were more severe and pronounced in mice infected with loop 4 mutants. Mutations in loop 1 and loop 2 of OmpA rendered the *E. coli* K1 unable to cause brain damage in mice and therefore appeared similar to control uninfected mice. The results are representative of five independent experiments with 12 animals per group. Scale bars, 20 μ m.

interact with different immune cells and examine whether specific regions are necessary for the onset of neonatal meningitis.

Computer modeling studies on OmpA structure have shown that the extracellular loops are highly mobile, and specific inter-loop interactions are critical for maintaining the three-dimensional structure of OmpA (49). Therefore, deletion of any loop would distort the three-dimensional structure of OmpA on *E. coli* K1. To avoid gross changes in the structure of OmpA, we generated mutants of OmpA in which three or four amino acids at a time have been exchanged for alanines. Although it was our aim to utilize the “alanine scanning method” to sequentially change the amino acids to alanines in OmpA, some of the mutations were found to be lethal to the bacteria. Therefore, only nine OmpA mutants were

generated and demonstrated to have no adverse effects to the phenotypic characteristics such as type 1 fimbriae and S-fimbriae expression, hemolysin, and polysaccharide production. The structures were also modeled, and their interaction with the receptor was examined to ensure that their structures did not distort significantly (37). In addition, the invasion studies in HBMEC with these mutants demonstrated that regions of loops 1, 2, and 4 are important for invasion (37). Prediction of OmpA interaction with GlcNAc1–4GlcNAc epitopes of Ecgp96 based on the molecular modeling correlated >99% with experimental data validating our computer modeling studies (37). Because our previous studies demonstrated that greater amounts of C4bp in serum prevented the entry of *E. coli* K1 into HBMEC (18), we speculated that C4bp might be binding to the regions similar to those of the OmpA receptor Ecgp96. In this study, we demonstrated that loop regions 1, 2, and loop 4 are critical for binding to C4bp, a classical complement pathway regulator, which has been shown to be responsible for bacterial evasion of serum complement activity (16, 17). This result also confirms our prediction that C4bp and Ecgp96 compete with each other for the same binding site on OmpA. Of note, loop regions 1–3 are necessary for survival in neutrophils similar to their role in interactions with HBMEC. Of note, we also observed that gp96, a homologue of Ecgp96, acts as a receptor on neutrophils for bacterial entry and survival inside the cells.³ In contrast, loops 2 and 3 played a major role in the survival of *E. coli* K1 in DCs. Although we have shown that *E. coli* infection induces CD47 expression in DCs, it is not clear at this time whether OmpA binds to CD47 or gp96 for survival in DCs (23). Furthermore, the survival of loop 1 and 3 mutants was significantly reduced in macrophages. We have demonstrated that OmpA interacts with the Fc- γ receptor I to bind to and enter the cells, which induced survival mechanisms in macrophages (21, 22).³ Entrance through other receptors such as CR3 caused the bacterial degradation inside macrophages. Of note, greater expression of gp96 was also observed in macrophages, along with Fc- γ receptor I and TLR2 upon infection with *E. coli* K1 both *in vitro* and *in vivo* (21, 22). Thus, the binding affinity of OmpA to Fc- γ receptor I could be greater than the binding to gp96 in macrophages. Based on these results, *E. coli* K1 must be evading complement attack by hiding inside neutrophils, DCs, and/or macrophages while undergoing replication before release into the blood, where the greater numbers of *E. coli* K1 neutralize the complement attack by depleting various complement components. Alternatively, lack of threshold levels of C4bp in premature neonates allows *E. coli* K1 to enter and survive inside immune cells and therefore results in high susceptibility for *E. coli* K1 infection.

Interestingly, in this study we observed that mutations in loop 4 induced elevated levels of immune response and influx of various immune cells into brain. Given a log increase in the number of bacteria in blood at 6 h post-infection, it is possible that loop 4 mutants may be avoiding initial serum killing and thus multiply faster. We have previously shown that neonatal

³ R. Mittal and N. V. Prasadarao, unpublished data.

serum kills *E. coli* K1 at or below 10^3 CFU/ml concentrations within 30 min *in vitro* (16). As the loop 4 mutant showed no significant increase in multiplication in immune cells compared with the wild type *E. coli* K1, it is likely that some serum complement components could not bind loop 4 mutants to kill the bacteria and thus initially avoid serum bactericidal activity. In summary, our studies demonstrated the involvement of various loops of OmpA in the interaction with different cell types and proteins during the establishment of disease. Because the loop 2 region appears to be participating in the majority of these interactions and its sequence similarity with allele *ompA2*, which has been shown to present in pathogenic bacteria, targeting loop 2 regions for immunization would be a possible therapeutic option for prevention of this deadly disease.

REFERENCES

- Nudelman, Y., and Tunkel, A. R. (2009) *Drugs* **69**, 2577–2596
- van de Beek, D., Drake, J. M., and Tunkel, A. R. (2010) *N. Engl. J. Med.* **362**, 146–154
- Croxen, M. A., and Finlay, B. B. (2010) *Nat. Rev. Microbiol.* **8**, 26–38
- Houdouin, V., Bonacorsi, S., Bidet, P., Blanco, J., De La Rocque, F., Cohen, R., Aujard, Y., and Bingen, E. (2008) *Clin. Microbiol. Infect.* **14**, 685–690
- Kaper, J. B., Nataro, J. P., and Mobley, H. L. (2004) *Nat. Rev. Microbiol.* **2**, 123–140
- Kim, K. S. (2010) *Lancet Infect. Dis.* **10**, 32–42
- Dubois, D., Prasadarao, N. V., Mittal, R., Bret, L., Roujou-Gris, M., and Bonnet, R. (2009) *Emerg. Infect. Dis.* **15**, 1988–1990
- Boyer-Mariotte, S., Duboc, P., Bonacorsi, S., Lemeland, J. F., Bingen, E., and Pinquier, D. (2008) *J. Antimicrob. Chemother.* **62**, 1472–1474
- Sidjabat, H. E., Derrington, P., Nimmo, G. R., and Paterson, D. L. (2010) *J. Antimicrob. Chemother.* **65**, 1301–1303
- Kim, K. S. (2003) *Nat. Rev. Neurosci.* **4**, 376–385
- Huang, S. H., Wass, C., Fu, Q., Prasadarao, N. V., Stins, M., and Kim, K. S. (1995) *Infect. Immun.* **63**, 4470–4475
- Kim, K. S. (2000) *Subcell. Biochem.* **33**, 47–59
- Prasadarao, N. V., Wass, C. A., Weiser, J. N., Stins, M. F., Huang, S. H., and Kim, K. S. (1996) *Infect. Immun.* **64**, 146–153
- Prasadarao, N. V. (2002) *Infect. Immun.* **70**, 4556–4563
- Prasadarao, N. V., Wass, C. A., and Kim, K. S. (1996) *Infect. Immun.* **64**, 154–160
- Prasadarao, N. V., Blom, A. M., Villoutreix, B. O., and Linsangan, L. C. (2002) *J. Immunol.* **169**, 6352–6360
- Wooster, D. G., Maruvada, R., Blom, A. M., and Prasadarao, N. V. (2006) *Immunology* **117**, 482–493
- Maruvada, R., Blom, A. M., and Prasadarao, N. V. (2008) *Immunology* **124**, 265–276
- Mittal, R., and Prasadarao, N. V. (2008) *J. Immunol.* **181**, 2672–2682
- Sukumaran, S. K., Shimada, H., and Prasadarao, N. V. (2003) *Infect. Immun.* **71**, 5951–5961
- Mittal, R., Gonzalez-Gomez, I., Panigrahy, A., Goth, K., Bonnet, R., and Prasadarao, N. V. (2010) *J. Exp. Med.* **207**, 1307–1319
- Mittal, R., Gonzalez-Gomez, I., Goth, K. A., and Prasadarao, N. V. (2010) *Am. J. Pathol.* **176**, 1292–1305
- Mittal, R., Gonzalez-Gomez, I., and Prasadarao, N. V. (2010) *J. Immunol.* **185**, 2998–3006
- Vogel, H., and Jähnig, F. (1986) *J. Mol. Biol.* **190**, 191–199
- Pautsch, A., and Schulz, G. E. (1998) *Nat. Struct. Biol.* **5**, 1013–1017
- Pautsch, A., and Schulz, G. E. (2000) *J. Mol. Biol.* **298**, 273–282
- Arora, A., Abildgaard, F., Bushweller, J. H., and Tamm, L. K. (2001) *Nat. Struct. Biol.* **8**, 334–338
- Kleinschmidt, J. H. (2003) *Cell. Mol. Life Sci.* **60**, 1547–1558
- Smith, S. G., Mahon, V., Lambert, M. A., and Fagan, R. P. (2007) *FEMS Microbiol. Lett.* **273**, 1–11
- Kleinschmidt, J. H. (2006) *Chem. Phys. Lipids* **141**, 30–47
- Wang, Y. (2002) *Biochem. Biophys. Res. Commun.* **292**, 396–401
- Behr, M. G., Schnaitman, C. A., and Pugsley, A. P. (1980) *J. Bacteriol.* **143**, 906–913
- Braun, V., and Bosch, V. (1972) *Eur. J. Biochem.* **28**, 51–69
- Morona, R., Klose, M., and Henning, U. (1984) *J. Bacteriol.* **159**, 570–578
- Koebnik, R. (1999) *J. Bacteriol.* **181**, 3688–3694
- Koebnik, R. (1999) *J. Mol. Biol.* **285**, 1801–1810
- Pascal, T. A., Abrol, R., Mittal, R., Wang, Y., Prasadarao, N. V., and Goddard, W. A., 3rd. (2010) *J. Biol. Chem.* **285**, 37753–37761
- Subramanian, K., Shankar, R. B., Meenakshisundaram, S., Lakshmi, B. S., Williams, P. H., and Balakrishnan, A. (2008) *J. Appl. Microbiol.* **105**, 715–722
- Ling, M., Wen, Y. J., and Lim, S. H. (1998) *Blood* **92**, 4764–4770
- Sokurenko, E. V., Courtney, H. S., Ohman, D. E., Klemm, P., and Hasty, D. L. (1994) *J. Bacteriol.* **176**, 748–755
- Criss, A. K., and Seifert, H. S. (2008) *Cell. Microbiol.* **10**, 2257–2270
- Luo, Y., and Dorf, M. E. (2001) *Curr. Protoc. Immunol.* **3**, 20.1–20.6
- Mittal, R., Aggarwal, S., Sharma, S., Chhibber, S., and Harjai, K. (2009) *FEMS Immunol. Med. Microbiol.* **57**, 156–164
- Teng, C. H., Xie, Y., Shin, S., Di Cello, F., Paul-Satyaseela, M., Cai, M., and Kim, K. S. (2006) *Infect. Immun.* **74**, 5609–5616
- Power, M. L., Ferrari, B. C., Littlefield-Wyer, J., Gordon, D. M., Slade, M. B., and Veal, D. A. (2006) *Appl. Environ. Microbiol.* **72**, 7930–7932
- Torres, A. G., and Kaper, J. B. (2003) *Infect. Immun.* **71**, 4985–4995
- Torres, A. G., Jeter, C., Langley, W., and Matthyse, A. G. (2005) *Appl. Environ. Microbiol.* **71**, 8008–8015
- Fagan, R. P., Lambert, M. A., and Smith, S. G. (2008) *Infect. Immun.* **76**, 1135–1142
- Datta, D., Vaidehi, N., Floriano, W. B., Kim, K. S., Prasadarao, N. V., and Goddard, W. A., 3rd. (2003) *Proteins* **50**, 213–221